

Article

Research on Grooved Concrete Pavement Based on the Durability of Its Anti-Skid Performance

Mulian Zheng ^{1,*}, Yanjuan Tian ¹, Xiaoping Wang ² and Ping Peng ³

¹ Key Laboratory for Special Area Highway Engineering of Ministry of Education, Chang'an University, South Erhuan Middle Section, Xi'an 710064, China; chdtianyj@163.com

² Hunan Province Highway Design Limited Company, Changsha 410005, China; 2016021025@chd.edu.cn

³ Gansu Province Transportation Planning, Survey and Design Institute Limited Company, Lanzhou 730030, China; yannilb@126.com

* Correspondence: zhengml@chd.edu.cn; Tel.: +86-298-233-4846

Received: 17 April 2018; Accepted: 23 May 2018; Published: 30 May 2018



Abstract: The objectives of the present study are to investigate the anti-skid performance of concrete pavement and to attempt to enhance its durability by two different methods: using a longitudinally-transversely grooved (LT) form, and using a self-developed composite curing agent containing paraffin and Na₂SiO₃ as the main ingredients. The friction coefficient (μ) was measured by self-developed equipment to evaluate the anti-skid performance of samples with three different groove forms (LT, longitudinally grooved (L), and transversely grooved (T)). Abrasion tests were then carried out to evaluate the durability of the anti-skid performance. The results indicated that anti-skid performance of LT samples was approximately 46.2% greater than that of T samples, but its durability was not as significant as that of T samples. However, the resistance to abrasion could be improved by using the aforementioned curing agent. Comparisons were carried out between samples sprayed the curing agent and control samples without any curing agent under standard conditions. It was found that the application of the curing agent increased the anti-skid durability of concrete by 35.4%~47.8%, proving it to be a useful and promising technique.

Keywords: concrete pavement; anti-skid performance durability; self-developed equipment; self-developed composite curing agent; longitudinally-transversely grooved form

1. Introduction

For several years, the anti-skid performance of cement concrete pavement has been the focus of much interest and research. Particularly on rainy days, due to a decrease in the anti-skid property of wet concrete surfaces, vehicles would skid out of control, resulting in casualties, property damage, and other serious consequences [1–3]. To enhance the anti-skid durability of concrete pavement, traditional techniques of napping, embossing, and grooving, known as the first-, second-, and third-generation anti-skid technologies, respectively, are commonly employed [4,5]. Over one or two years, napping pavements are rapidly polished and as a result the skid resistance is gradually attenuated. Embossing, with poor maneuverability, contributes little to the anti-skid performance improvement. Currently, widespread use of newer anti-skid technologies including exposed aggregate, embedded aggregate [6,7], and porous pavement is hindered by many drawbacks such as high costs, process complexity, and requirement constraints [8]. The friction performance of grooved pavement is significantly higher than that of non-grooved pavement [9]. Grooves could provide better drainage channels and improve the pavement's anti-skid performance, reducing the number of traffic accidents, especially on rainy days [10–12].

In many countries in which the grooving of concrete pavement is the most commonly used anti-skid durability technology, groove dimensions, design, and evaluation are the primary research areas [13–15]. In the United States, skid resistance force is recognized as the critical indicator of grooved concrete pavement performance by the Portland Cement Association (PCA) and American Association of State Highway and Transportation Officials (AASHTO) [16]. These organizations have adopted equally spaced rectangular grooves, of a width greater than 3 mm, a depth less than 6 mm, and spacing varying between 12 and 25 mm. In France, it was shown that increasing the groove width or reducing the groove spacing could improve the anti-skid performance of the pavement under the conditions of certain grooved surface areas [17]. It was therefore recommended that concrete pavement should be formed with transverse, equally spaced, rectangular grooves with a width between 3 and 5 mm, a depth between 5 and 6 mm, and groove spacing of 20 to 30 mm. Fwa [18] adopted grooves with a width varying from 2 to 10 mm, a depth from 1 to 10 mm, and spacing from 5 to 25 mm. Lee [19] developed an automatic instrument to measure groove dimensions in field experiments, resulting in the enhanced efficiency of grooved pavement evaluation.

The use of transverse rectangular grooves, with equal spacing of 20 mm and width and depth varying from 3 to 5 mm, has been suggested for expressways and first-class highways in China [20]. Meanwhile, municipal and rural roads in our country feature transverse rectangular grooves with smaller dimensions than higher-class roads, with widths varying from 3 to 5 mm, depths from 1 to 6 mm, and spacing from 15 to 40 mm. Li [10] proposed a simulation method using finite element software to investigate groove parameters, thus determining the optimal dimensions for longitudinally grooved (L) and transversely grooved (T) samples to be 6 mm wide, 4 mm deep, and 10 mm in spacing. To provide the required friction force, domestic concrete pavement is generally formed with transverse grooves and a wide groove spacing of approximately 20 mm.

Currently, the most commonly used concrete pavement curing agents can be divided into inorganic and organic types. Inorganic curing agents can improve the strength of concrete and have the advantage of relatively low expenses. While the inadequate surface hydration of concrete leads to early cracks, the formation of the waterproof membrane on the concrete surface is incomplete after drying. The use of paraffin emulsion-type organic curing agents results in good water retention and a smooth waterproof membrane, but does not enhance the strength of the concrete surface.

In summary, while there has been minimal progress in the research and development of concrete pavement durability, groove technology has been applied worldwide. Research on this issue in China needs to be further conducted to develop high anti-skid performance pavement. Through the evaluation of durability, the primary purpose of this study is to further investigate anti-skid technologies for grooved pavement. To enhance the anti-skid performance, a longitudinally-transversely grooved (LT) technique and new curing method are proposed. Additionally, optimal groove dimensions for better anti-skid durability are recommended for practical applications according to the laboratory tests.

2. Materials and Methods

Selecting the raw materials and mixture proportions for the grooved concrete pavement was the first step in this study. The LT method was proposed next, and anti-skid tests were implemented on samples of two different forms to evaluate skid resistance. Subsequently, abrasion resistance tests were designed to evaluate the anti-skid durability. Finally, we developed a new curing agent and applied it to different groove samples. The following subsections describe the step-by-step methodology that was applied in detail.

2.1. Raw Materials

Cement, coarse aggregate, fine aggregate, and water were used in the concrete mixtures for this investigation. Table 1 displays the mix proportions for the grooved concrete pavement used in this study, and the water-to-cement (w/c) ratio and sand ratio were maintained at 0.46% and 34%, respectively [21]. The cement used was ordinary Portland cement (type P.O.42.5, China), with the

parameters listed in Table 2. The coarse aggregate was crushed limestone produced in Xianyang, China, and the fine aggregate including river sands were sourced from Bahe, China. Tables 3 and 4 display the parameters for the coarse and fine aggregates, respectively.

The self-developed concrete curing agent, adopted in the present study, has been patented (Patent no.: CN201410312792.6). It is mainly composed of Na_2SiO_3 (as the critical inorganic component) and paraffin wax (as the critical organic component). Its parameters are listed in Table 5.

Table 1. Mix proportions of grooved concrete pavement.

Items		Unit	Value
Concrete Strength Level		...	C30
Water to Cement Ratio		...	0.46
Sand Ratio		%	34
Mix Proportion	Cement	kg/m ³	411
	Crushed Limestone	kg/m ³	1212
	Sand	kg/m ³	624
	Water	kg/m ³	190

Table 2. Parameters of the cement.

Parameter	Unit	Value	
Cement Type	...	P.O.42.5	
Density	g/cm ³	3.2	
Specific Surface Area	m ² /kg	355	
Setting Time	Initial Set	min	215
	Final Set	min	270
Compressive Strength	3 days	MPa	27.6
	28 days	MPa	45.1
Flexural Strength	3 days	MPa	5.9
	28 days	MPa	7.8

Table 3. Parameters of the crushed limestone.

Parameter	Unit	Value	Conclusion
Apparent Density	g/cm ³	2.69	...
Loose Density	g/cm ³	1.47	...
Crushing Value	%	9.7	Qualified
Mud Content	%	0.827	Qualified
Elongated Articles	%	9.3	Qualified

Table 4. Parameters of the river sands.

Parameter	Unit	Value	Conclusion
Apparent Density	g/cm ³	2.628	...
Loose Density	g/cm ³	2.621	...
Fineness Modulus	%	2.365	...
Mud Content	%	1.407	Qualified
Moisture Content	%	2.876	Qualified

Table 5. Parameters of the agent.

Parameter	Unit	Value	Conclusion	
Effective Water Retention Rate	%	93.78	≥90	
Abrasion Loss	kg/m ²	2.365	≤3.0	
Solid Content	%	31.04	≥20	
Drying Time	h	0.6	≤4	
Compressive Strength Rate	7 days	min	105	≥95
	28 days	min	108	≥95

2.2. LT Method

The anti-skid force applied to vehicles mainly relates to the macro structure of the cement concrete pavement [22]. It can be increased by grooves, thus resulting in higher skid resistance in grooved compared to non-grooved pavement [23]. Grooved concrete pavements are commonly applied in two forms, L and T, and can effectively improve the skid resistance. In accordance with the aforementioned research and engineering practice, the T form is superior to the L form in terms of anti-skid performance, durability, driving comfort, direction control, and incidence of accidents [24]. Additionally, the L form is one constituent of the LT form. Thus, LT concrete pavement is proposed to provide greater braking performance to T, and to develop the advantages of both T and L pavement. Figure 1 shows a sketch of the LT form.

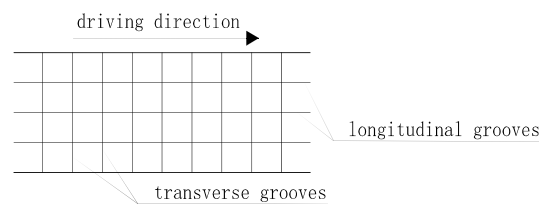


Figure 1. Sketch of the longitudinally-transversely grooved (LT) form.

2.3. Preparation of the Test Samples

Samples (300 mm × 300 mm × 50 mm) were prepared for the test. The aggregate was initially mixed with dry cement for 60 s to improve the bond between the aggregate and cement paste, before gradually mixing in the remaining water over 90 s, and then casting. After being cured for 24 h in a fog room at 20 ± 2 °C and 95% relative humidity [25], the samples were demolded. A cutting machine was used to create grooves in the concrete after it had been cured for 3 to 4 days [26]. To ensure that the grooves were straight and uniform, lines were drawn on the test samples in accordance with the design requirements. As shown in Figure 2, a straight board was placed on the test samples and used as the guide rail for the cutting machine.

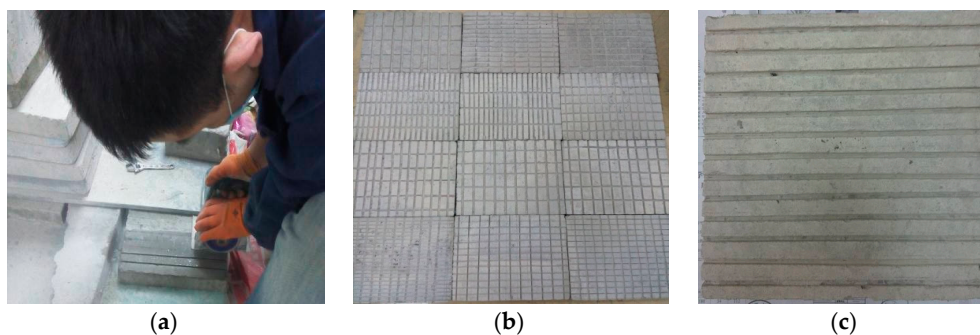


Figure 2. These images show the preparation of the test samples. (a) The grooving technology and process; (b,c) the grooved test samples.

2.4. Anti-Skid Tests

The dynamic rotating friction coefficient tester developed by the research team, which has been patented (Patent no.: CN200820222395.X), was used to measure the anti-skid performance of the samples (shown in Figures 3 and 4). It was operated by installing a test slide sample under a certain load on the test disc, then placing the test disc onto the pavement. When the disc is rotated at a given speed, the torque required to drive the disc is obtained from the driving engine. The friction coefficient of the pavement surface is calculated according to Equation (1):

$$\mu = \frac{N}{dG} \tag{1}$$

where μ is the friction coefficient of the pavement surface, N is the torque required to drive the disc, d is the friction arm (10 cm), and G is the vertical load (21.56 N).

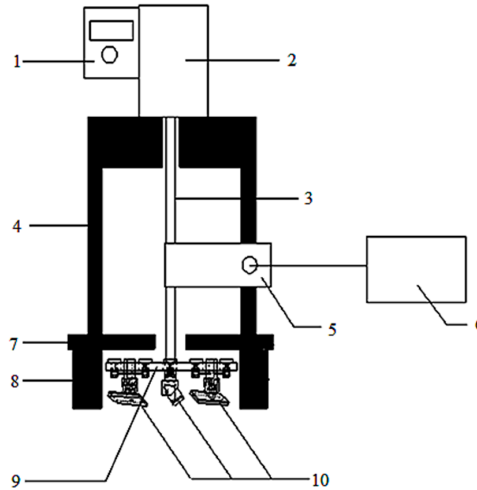


Figure 3. Sketch of the dynamic rotating friction coefficient tester. The tester includes the following: (1) speed control device, (2) engine, (3) axis of rotation, (4) shell, (5) torque sensor, (6) digital display instrument, (7) weighing plate, (8) bearing, (9) test disc, and (10) rubber slider.

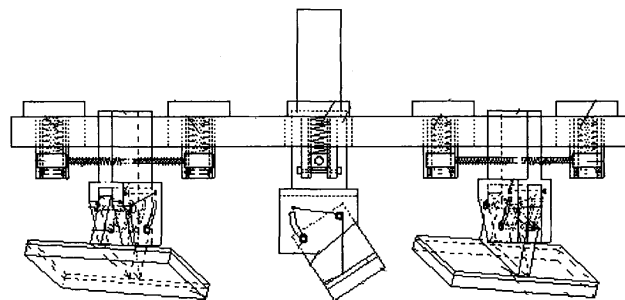


Figure 4. Image of the test disc of the dynamic rotating friction coefficient tester.

The texture depth (TD), the British Pendulum Number (BPN), and the friction coefficient (μ) methods are all commonly used to evaluate the anti-skid performance of pavement. Table 6 shows the Chinese code performance requirements [20]. Of these methods, the TD method is the most suitable for evaluating concrete pavement. Hence, the μ , adopted to evaluate the anti-skid performance in this paper, needed to be converted to TD in the laboratory tests.

Table 6. Anti-skid requirements for concrete pavement ¹.

Road Section		Acceptance Value of TD (The Texture Depth)	Unit
Expressway, First-Class	General Road Section	0.7~1.10	mm
Highway	Special Road Section	0.8~1.20	mm

¹ Table 6 references Table 7.2.2 in China code *Inspection and Evaluation Quality Standards for Highway Engineering Section 1 Civil Engineering (JTG F80/1-2017)*.

Table 6 shows the anti-skid requirements for concrete pavement, where special road section refers to interchanges, grade crossings, and speed change lanes of expressways and first-class highways.

Contrast tests, using nine samples, were implemented between the dynamic rotating friction coefficient tester method and the sand-laying method [27]. The test results are shown in Table 7.

Table 7. The results of the anti-skid tests.

Sample No.	TD/mm	μ
1	0.91	0.63
2	1.02	0.64
3	0.89	0.56
4	0.97	0.59
5	1.09	0.74
6	0.9	0.60
7	1.24	0.78
8	1.02	0.80
9	1.01	0.69

The regression equation was obtained by the data in Table 7, as shown in Equation (2).

$$\mu = \frac{TD - 0.8904}{3.7599TD^2 - 2.9579} + 0.5427TD (R = 0.8863) \tag{2}$$

As seen in Equation (2), μ and TD are positively correlated. By using the conversion relation of μ and TD , the results of μ should meet the specified requirements shown in Table 8.

Table 8. Anti-skid requirements for concrete pavement.

Road Section	Acceptance Value of μ
Expressway, First-Class Highway	General Road Section ≥ 0.55 Special Road Section ≥ 0.60

In order to compare and analyze the effects of different grooved forms on skid resistance, two types (T and LT) of grooved samples were prepared to implement comparative anti-skid tests.

2.4.1. T Schemes

In accordance with previous studies and experience, the T concrete pavement had better skid resistance when the groove width was 6 mm [10,11]. With this consistent width, samples with three different depths (2, 4, and 6 mm) and three different spacing arrangements (10, 20, and 30 mm) were prepared in this investigation, as shown in Table 9.

Table 9. Sample dimensions schemes.

Sample No.	T (Transversely Grooved) Width/mm	T Depth/mm	T Spacing/mm
1	6	2	10
2	6	2	20
3	6	2	30
4	6	4	10
5	6	4	20
6	6	4	30
7	6	6	10
8	6	6	20
9	6	6	30

2.4.2. LT Schemes

Larger groove dimensions were adopted in this study in order to select the appropriate LT sample. Table 10 shows the influence of the six factors on LT groove dimensions. In accordance with the orthogonal experimental design methodology [28], the groove dimensions were prepared in $L_{25}(5^6)$.

Table 10. Levels of factors (cm).

Level	T Width (A)	T Depth (B)	T Spacing (C)	L (Longitudinally Grooved) Width (D)	L Depth (E)	L Spacing (F)
k1	2	2	15	2	2	10
k2	3	3	30	3	3	17
k3	4	4	45	4	4	24
k4	5	5	60	5	5	31
k5	6	6	75	6	6	37

2.4.3. Comparative Analysis of Different Groove Forms

To evaluate differences in skid resistance, a comparative analysis was conducted between the two best-performing T and LT grooved samples in the above anti-skid tests.

2.5. Skid Resistance Test

In accordance with the Chinese code, the abrasion resistance test by an abrasion tester was used to evaluate the anti-skid durability of the concrete samples [25]. The test operation process was as follows. Each sample was placed on a horizontal turntable of the abrasion tester, as shown in Figure 5, and fastened by the clamp. Samples, loaded 200 N, were ground for 30 revolutions, then removed, and weighed after brushing the grinding dust from the sample’s surface. Meanwhile, the corresponding quality (m_1) of the sample was recorded as the initial quality. In order to promptly remove dust during the grinding process, a vacuum cleaner was aligned with the abraded surface of the samples. Each set of blades was used for one sample group test, and was replaced with a new set of blades before testing the next group.

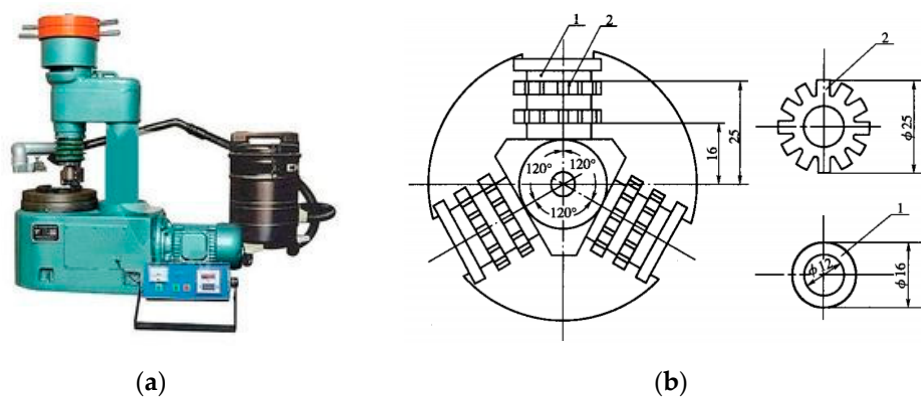


Figure 5. Picture of the abrasion tester. (a) Photo of the abrasion tester; (b) sketch of the grinding blades. In (b), 1 is a gasket and 2 is a blade.

Abrasion loss per unit area of each sample was calculated by Equation (3) with an accuracy of 0.001 kg/m^2 .

$$G = \frac{m_1 - m_2}{0.0125} \tag{3}$$

where G is the abrasion loss per unit area (kg/m^2), m_1 is the original quality, m_2 is the quality after abrasion (kg), and 0.0125 is the abrasion area (m^2).

2.5.1. Evaluation of the Grooved Samples

The samples exhibiting the best skid resistance in the aforementioned tests (the two best-performing T and LT samples) were subjected to the abrasion resistance tests to identify the differences in their skid resistance durability. In particular, each dimension sample was produced in two groups, and the mean value was adopted as the final result.

2.5.2. Evaluation of Samples under Different Curing Methods

The various curing methods have different effects on the abrasion resistance of concrete pavement. In this study, a composite curing agent, containing Na_2SiO_3 and paraffin as the primary ingredients, was self-developed to improve the concrete performance [20]. This agent has the properties of high water retention, strength, and abrasion resistance, as listed in Table 5. This paper investigated the abrasion resistance of grooved concrete under different curing methods.

The authors prepared eight accordant samples with the sample dimensions (300 mm × 300 mm × 50 mm) that offered the best skid resistance (the two best-performing T and LT samples) in the above tests, and then divided them into two groups. One group was adopted as the control group (without any curing agent), cured in standard curing box ($20\text{ }^\circ\text{C} \pm 1\text{ }^\circ\text{C}$, relative humidity >90%, maintenance water $20\text{ }^\circ\text{C} \pm 1\text{ }^\circ\text{C}$) for 28 days [25]. The other group was sprayed with the curing agent at a spraying dose of 0.22 kg/m^2 , with an inorganic to organic curing ratio of 4:6. The samples were sprayed for a second time with the same preparation 30 min later. After spraying twice, the samples were cured for 28 days under conditions identical to those of the control group. Subsequently, all samples were dried at room temperature, and surface dust was brushed away. The abrasion tester shown in Figure 5 was used to conduct abrasion resistance tests. And the abrasion loss per sample was measured and recorded; the mean value of four samples was calculated and adopted as the final result.

After the cement concrete mixture was poured, the inorganic ingredient was sprayed into the mold approximately 4 to 6 h after surface exudation. Thirty minutes later, the organic ingredient was applied by spraying between $20\text{ }^\circ\text{C}$ and $30\text{ }^\circ\text{C}$ (room temperature). The curing agent applied to the sample's surface was sprayed uniformly, and the dose was strictly controlled. Figure 6 shows the sample after spraying the curing agent.



Figure 6. Appearance after spraying the composite curing agent.

The samples were cured, after demolding, for 24 h under standard conditions. A curing film was applied to each surface except the grooved surface. Three or four days after grooving, the grooved surface was sprayed with the curing agent, while the other surfaces were still undergoing the film curing processing. Figure 7 shows a sample sprayed with the composite curing agent after grooving.



Figure 7. Photo after spraying the composite curing agent after grooving.

3. Results and Conclusions

This section presents the anti-skid performance and abrasion resistance results for the different grooved samples, and analyzes the impact of the curing agent on the anti-skid durability of the concrete pavement.

3.1. Results of Anti-Skid Tests

3.1.1. Anti-Skid Results for T Schemes

Table 11 shows μ for the T samples, determined by measuring skid resistance.

Table 11. Results of skid-resistant performance for L samples.

Sample No.	1	2	3	4	5	6	7	8	9
μ	0.63	0.58	0.63	0.56	0.82	0.46	0.57	0.65	0.61

According to Table 11, μ is maintained within a certain range, as influenced by the groove dimensions. As the groove width becomes larger, the groove quality improves, but μ is reduced as the groove spacing and depth increase, with no clear correlation. This is because as the groove width increases, the area of tire embedding in the groove also increases; so, while increasing the groove depth enhances the tire plowing effect, the surface resistance of the groove is improved. When the groove spacing is small, the tire/pavement plowing effect is enhanced, thus improving pavement skid resistance.

According to the principles of skid resistance measurement, the μ of T and L samples was the same. Our test results indicated that T (L) samples 5 (6, 4, 20 mm) and 8 (6, 6, 20 mm) had the greatest skid resistance.

3.1.2. Anti-Skid Results for LT Schemes

Table 12 illustrates the skid resistance performance results for LT samples, and Table 13 displays the range analysis of LT samples. k_{ij} in Table 13 refers to the average value of the sum of μ in the j column under the k_i level; R_j refers to the difference between the maximum value and minimum value of k_{1j} , k_{2j} , k_{3j} , k_{4j} , and k_{5j} in the j column, namely, range. The size of range represents the different effects of each factor on the μ value. Figure 8 shows the range analysis chart of the six factors.

Table 12. Skid-resistant performance of LT samples.

Sample No.	1	2	3	4	5	6	7	8	9	10
μ	0.758	0.623	0.573	0.544	0.528	0.574	0.919	0.863	0.505	0.727
Sample No.	11	12	13	14	15	16	17	18	19	20
μ	0.696	0.492	0.756	1.039	0.772	0.949	0.567	0.904	1.200	0.609
Sample No.	21	22	23	24	25					
μ	0.824	1.157	0.652	0.586	0.797					

Table 13. Range analysis of LT samples ².

Level	A	B	C	D	E	F
k1	0.605	0.760	0.917	0.636	0.709	0.886
k2	0.718	0.752	0.764	0.728	0.705	0.792
k3	0.751	0.750	0.677	0.710	0.763	0.791
k4	0.846	0.775	0.729	0.793	0.728	0.637
k5	0.605	0.760	0.917	0.636	0.709	0.886
Range	0.241	0.088	0.281	0.253	0.112	0.269
Factors in Primary and Secondary Order	C > F > D > A > E > B					
Optimal Scheme	C1F1D5A4E5B4					

² Where A is T width, B is T depth, C is T spacing, D is L width, E is L depth, and F is L spacing.

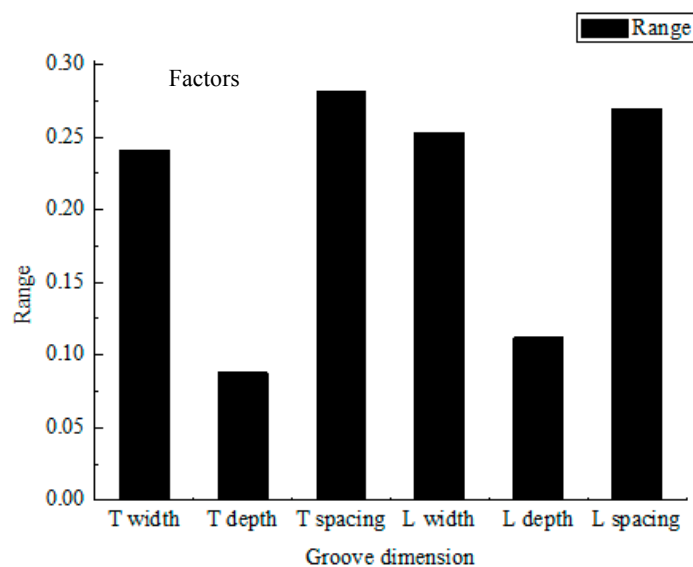


Figure 8. Columnar analysis diagram of the range analysis of LT samples.

The range analysis of LT samples shown in Table 13 and Figure 8 indicates that T spacing is the key factor impacting the anti-skid performance of concrete pavement, followed by L spacing, L width, T width, L depth, and T depth. The groove volume within a certain scope is the primary factor affecting μ . The results of mathematical calculations and experimental findings are slightly different, but remain consistent throughout the geometric analysis. Finally, the test results show that LT samples 19 (5, 5, 30, 6, 4, 10 mm) and 22 (6, 3, 15, 6, 5, 24 mm) have the greatest skid resistance.

3.1.3. Comparative Analysis of Test Results for Different Groove Forms

Table 14 shows results for the two best-performing T and LT grooved samples in the above anti-skid tests.

Table 14. Results of skid-resistant testing for different samples (mm).

Samples Dimensions	(6, 4, 20)	(6, 6, 20)	(5, 5, 30, 6, 4, 10)	(6, 3, 15, 6, 5, 24)
μ	0.821	0.651	1.200	1.157

As can be seen in Table 14, μ of LT samples (5, 5, 30, 6, 4, 10) is approximately 46.2% greater than that of T samples (6, 4, 20). The anti-skid performance of the LT samples used in this experiment is significantly better than that of the T samples.

It can be seen that groove forms have a very important influence on anti-skid performance, and that LT schemes can effectively improve the anti-skid performance of pavement. It can be inferred that the embedded squeeze effect of the tire-road interface, the effective contact area, and the resistance to change all increase as the groove number increases; therefore, the sliding resistance increases.

3.2. Results of Abrasion Resistance Tests

3.2.1. Results for Grooved Samples

Table 15 shows the abrasion test results for the grooved samples.

Table 15. Abrasion loss of different grooved samples (kg/m²).

Sample Dimensions	(6, 4, 20)	(6, 6, 20)	(6, 3, 15, 6, 5, 24)	(5, 5, 30, 6, 4, 10)
G _c (kg/m ²)	3.17	3.28	4.56	3.69

From Table 15, it can be seen that the abrasion loss of sample (6, 4, 20) is the smallest of the four different samples; that of sample (6, 3, 15, 6, 5, 24) is the largest, but the difference between them is relatively small. This indicates that the anti-skid performance of the LT samples was improved, but the durability performance was not.

It is inferred that the improved tire-road friction is due to the grid formed by the LT form, which increases the number of prominent corners. Road surface abrasion resistance gradually decreases because of the continuous vehicle loads.

3.2.2. Results of Using the Curing Agent

Table 16 shows the results of the abrasion resistance tests for the samples using different curing methods.

Table 16. Abrasion loss for different curing methods (kg/m²).

Samples Dimensions	Standard Method without Agent	Spraying Curing Agent
(6, 4, 20)	3.17	1.83
(6, 6, 20)	3.28	2.12
(6, 3, 15, 6, 5, 24)	4.56	2.38
(5, 5, 30, 6, 4, 10)	3.69	1.97

As shown in Table 16, the use of the curing agent improves the abrasion resistance of grooved samples by 35.4%~47.8%. The concrete curing agent itself could improve both strength and abrasion resistance; therefore, the strength and abrasion resistance of the sprayed grooved samples were greatly enhanced. In addition, the humidity during the curing and improvement in the overall strength of the sample was ensured by covering the grooved surface and other surfaces with a plastic film.

In conclusion, the application of this curing agent results in improved abrasion resistance performance in grooved concrete, and is an advisable and promising technique to improve the anti-skid performance and durability of such surfaces.

4. Conclusions

This study provides an experimental investigation of the anti-skid performance and abrasion resistance of cement concrete pavements, including the LT grooved method, the curing method using a composite curing agent, anti-skid tests, and abrasion resistance tests. These tests were performed on samples with different grooved schemes, and conclusions could be drawn as follows:

- (1) The two techniques used in this study, including LT grooving and a curing method using a composite concrete curing agent, could effectively enhance the anti-skid performance of the pavement.
- (2) From the experimental study of the anti-skid performance of concrete pavement with different groove schemes, LT had relatively good skid resistance compared to other schemes.
- (3) The improvement in durability observed for concrete cured using the sprayed composite curing agent indicates that this can be an effective method to maintain concrete pavement in practical applications.
- (4) Based on the results of skid and abrasion resistance tests, the longitudinally-transversely grooved sample (5, 5, 30, 6, 4, 10) provides better skid resistance and durability and can be suggested to be adopted as the optimal dimensions for good anti-skid durability for concrete pavement. This sample's dimensions, including transverse groove width, transverse groove depth, transverse groove spacing, longitudinal groove width, longitudinal groove depth, and longitudinal groove spacing, were 5, 5, 30, 6, 4, and 10 mm, respectively.

Author Contributions: M.Z. conceived and designed the experiments; Y.T. performed the experiments and analyzed the data; X.W. and P.P. contributed reagents and materials; M.Z. wrote the paper.

Acknowledgments: This research was supported by the Fundamental Research Funds for the Central Universities in China (No. 310821163502), the Transportation Department of Hebei Province (Grant No. T-2012107 and Y-2012014), the Transportation Department of Jiangxi Province (Grant No. Ganjiaokejiao [2015]), and the Transportation Department of Hubei Province of China (No. Ejjiaokejiao [2012] 857). In addition, the authors would like to thank the reviewers of this paper for their ever-present support and valuable advice.

Conflicts of Interest: The authors declare no conflict of interest.

References

1. Yang, X.D.; Zheng, M.L.; Zhu, H.T.; Li, Z.Z.; Wang, B.G. Numerical analysis of frictional contact condition between tire and cement concrete pavement. *J. Chang'an Univ. (Nat. Sci. Ed.)* **2010**, *30*, 13–17.
2. Liu, Y.; Tian, B.; Niu, K.M. Research on skid resistance and noise reduction properties of cement concrete pavements with different surface textures. *J. Highw. Transp. Res. Dev. (Eng. Ed.)* **2013**, *7*, 22–27. [[CrossRef](#)]
3. José, M.; Pardillo, M.; Rafael, J.P. An assessment of the skid resistance effect on traffic safety under wet-pavement conditions. *Accid. Anal. Prev.* **2009**, *41*, 881–886.
4. Wang, L.L.; Zhang, J.X.; Zhang, C.; Zhao, E.Q. Discussion about anti-skid changing-laws of cement concrete pavement. *Highw. Eng.* **2008**, *33*, 5–8.
5. Liu, Y.; Tian, B.; Niu, K.M. Skid-resistance and denoising properties of cement concrete pavement with different surface texture. *J. Highw. Transp. Res. Dev.* **2012**, *29*, 28–33.
6. Song, Y.C.; Fu, B.F.; Liang, N.X. Comprehensive evaluation of surface function of exposed-aggregate cement concrete pavement. *J. Chongqing Jiaotong Univ. (Nat. Sci. Ed.)* **2015**, *34*, 43–47.
7. Wang, F.Z.; Yang, L.; Wang, H.; Yu, H.G. Facile preparation of photo catalytic exposed aggregate concrete with highly efficient and stable catalytic performance. *Chem. Eng. J.* **2015**, *264*, 577–586. [[CrossRef](#)]
8. Chen, Y.; Wu, X.Y. Fractal features and surface texture parameters of porous cement concrete pavement. *J. Changsha Univ. Sci. Technol. (Nat. Sci. Ed.)* **2007**, *4*, 13–17.
9. Zhu, S.Z.; Huang, X.M. Numerical simulation of tire hydroplaning speed on transverse grooved concrete pavements. *J. Southeast Univ. (Nat. Sci. Ed.)* **2016**, *46*, 1296–1300.
10. Li, B.; Han, S. Review on the selection of the parameters of the concrete pavement at home and abroad. *East China Highw.* **2010**, *2*, 81–82.

11. Huo, M. *Research on Skid Resistance Function Attenuation and Evaluation Method of Cement Concrete Pavement*; China Architecture and Building Press: Beijing, China, 2011.
12. Han, S.; Li, N.; Li, B.; Huo, M.; Han, W.W. Tests study on skid resistance attenuation of cement concrete pavement. *J. Guangxi Univ. (Nat. Sci. Ed.)* **2010**, *35*, 896–900.
13. Wang, K.; Lin, L.; Li, Q.J.; Nguyen, V.; Hayhoe, G.; Larkin, A.L. Runway groove identification and evaluation using 1 mm 3D image data. In Proceedings of the Airfield and Highway Pavement Conference, Los Angeles, CA, USA, 9–12 June 2013; pp. 730–741.
14. Alexandre, L.O.; Luiz, R.P.J. Evaluation of the superficial texture of concrete pavers using digital image processing. *J. Constr. Eng. Manag.* **2015**, *141*, 04015034. [[CrossRef](#)]
15. Kelvin, C.P.W.; Luo, W.T.; Joshua, Q.L. Hydroplaning risk evaluation of highway pavements based on IMU and 1 mm 3D texture data. In *Transportation and Development Institute Congress 2nd. 2014 (T&DI 2014)*; ASCE: Reston, VA, USA, 2014; pp. 511–522. [[CrossRef](#)]
16. Lee, Y.P.K.; Liu, Y.R.; Liu, Y.; Fwa, T.F.; Choo, Y.S. Skid resistance prediction by computer simulation. *Appl. Adv. Technol. Transp. Eng.* **2004**, 465–469. [[CrossRef](#)]
17. Scott, H.R.; Joseph, R.R.; John, J.H. Criteria for predicting hydroplaning potential. *J. Transp. Eng.* **1986**, *112*, 549–553. [[CrossRef](#)]
18. Fwa, T.F.; Ong, G. Transverse pavement grooving against hydroplaning. II: Design. *J. Transp. Eng.* **2006**, *132*, 449–457. [[CrossRef](#)]
19. Lee, M.H.; Chou, C.P.; Li, K.H. Automatic measurement of runway grooving construction for pavement skid evaluation. *Autom. Constr.* **2009**, *18*, 856–863. [[CrossRef](#)]
20. MOT (Ministry of Transportation). *Technical Guideline for Construction of Highway Cement Concrete Pavements (JTG/T F30-2014)*; China Communication Press: Beijing, China, 2014.
21. MOHURD (Ministry of Housing and Urban-Rural Development). *Specification for Mix Proportion Design of Ordinary Concrete (JGJ 55-2011)*; China Architecture and Building Press: Beijing, China, 2011.
22. Wen, S.T.; Huang, P. *Principles of Tribology*, 4th ed.; Tsinghua University Press: Beijing, China, 2010; ISBN 978-7-302-30188-2.
23. MOHURD (Ministry of Housing and Urban-Rural Development). *Code for Concrete Admixture Application (GB 50119-2013)*; China Architecture and Building Press: Beijing, China, 2013.
24. MOHURD (Ministry of Housing and Urban-Rural Development). *Standard for Test Method of Mechanical Properties on Ordinary Concrete (GB/T 50081-2002)*; China Architecture and Building Press: Beijing, China, 2002.
25. MOT (Ministry of Transportation). *Test Methods of Cement and Concrete for Highway Engineering (JTG E30-2005)*; China Communication Press: Beijing, China, 2005.
26. MOT (Ministry of Transportation). *Technical Specification for Construction of Highway Concrete Pavement (JTG F30-2003)*; China Communication Press: Beijing, China, 2003.
27. MOT (Ministry of Transportation). *Field Test Methods of Subgrade and Pavement for Highway Engineering (JTG E60-2008)*; China Communication Press: Beijing, China, 2008.
28. Li, Y.Y.; Hu, C.R. *Experiment Design and Data Processing*; Chemical Industry Press: Beijing, China, 2008.



© 2018 by the authors. Licensee MDPI, Basel, Switzerland. This article is an open access article distributed under the terms and conditions of the Creative Commons Attribution (CC BY) license (<http://creativecommons.org/licenses/by/4.0/>).